Nuclear Instruments and Methods in Physics Research A 696 (2012) 141–143

Contents lists available at SciVerse ScienceDirect

Nuclear Instruments and Methods in Physics Research A

journal homepage: www.elsevier.com/locate/nima

Letter to the Editor

Angular distribution of X-ray transition radiation from regular radiators

V.M. Grichine [a,b]

[a] Lebedev Physical Institute, Moscow, Russia
[b] CERN, Geneva, Switzerland

ARTICLE INFO

Article history:
Received 11 August 2012
Received in revised form
1 September 2012
Accepted 2 September 2012
Available online 8 September 2012

Keywords:
X-rays transition radiation
Angular distribution

ABSTRACT

Algorithm for the angular distribution of X-ray transition radiation generated by a relativistic charged particle in regular radiators is discussed in the framework of the Geant4 simulation toolkit. The model predictions are compared with experimental data sensitive to the angular distribution of X-ray transition radiation.

X-ray transition radiation (XTR) is widely used in experimental high energy physics for charged particle identification, especially for the selection of electrons in an environment of high hadron background [1]. Two of the CERN LHC experiments, ATLAS [2] and ALICE [3], have XTR detectors for the particle identification. XTR is emitted in a very forward region relative to the charged particle track and the XTR energy spectrum is usually measured together with ionization background produced by the charged particle. It is, however, possible to measure the XTR spectrum itself in detectors with high space resolution like high pressure gaseous detectors [1] or silicon detectors with strip and pad readout [4,5]. The goal of this letter is to describe algorithm allowing one to simulate the XTR angular distribution for experimental setups with high space resolution XTR detectors in the framework of the Geant4 toolkit [6]. Since the charged particle experiences multiple scattering it is convenient to use the Geant4 XTR models based on the approach of the radiation energy loss, since in this case the XTR angle is counted from the current particle direction corresponding to the region of the XTR origin inside multilayer XTR radiator.

Using the methods developed in Refs. [7–9] one can derive the relation describing the mean number of XTR photons, $\overline{N}_{in}$, generated by relativistic charge e per unit photon frequency ω and emitting (relative to the charge direction) angle squared θ^2, $d^2\overline{N}_{in}/d\omega\, d\theta^2$, inside radiator consisting of n foils of the first ($j=1$) medium interspersed with gas gaps of the second ($j=2$) medium with fluctuating gap thicknesses t_j:

$$\frac{d^2\overline{N}_{in}}{d\omega\, d\theta^2}=\frac{2\alpha}{\pi c^2}\omega\theta^2\mathrm{Re}\{\langle R^{(n)}\rangle\},\quad H=H_1H_2 \tag{1}$$

$$\langle R^{(n)}\rangle=(Z_1-Z_2)^2\left\{n\frac{(1-H_1)(1-H_2)}{1-H}+\frac{(1-H_1)^2H_2(1-H^n)}{(1-H)^2}\right\}$$

where α is the fine structure constant. In the case of often used gamma distributed gap thicknesses t_j the correlation factors H_j can be expressed as simple analytical expression:

$$H_j=\int_0^\infty dt_j\left(\frac{\nu_j}{\overline{t}_j}\right)^{\nu_j}\frac{t_j^{\nu_j-1}}{\Gamma(\nu_j)}\exp\left[-\frac{\nu_j t_j}{\overline{t}_j}-i\frac{t_j}{2Z_j}\right]=\left[1+i\frac{\overline{t}_j}{2Z_j\nu_j}\right]^{-\nu_j} \tag{2}$$

where Γ is the Euler gamma function, $\overline{t}_j$ is the mean thickness of the j-th medium in the radiator and $\nu_j>0$ is the parameter roughly describing the relative fluctuations of t_j. In fact, the relative fluctuation of t_j is, $\delta_j=1/\sqrt{\nu_j}$. The complex formation zone of XTR in the j-th medium [7,10], Z_j ($j=1,2$) is defined by

$$Z_j=\frac{L_j}{1-i\frac{L_j}{l_j}},\quad L_j=\frac{c}{\omega}\left[\gamma^{-2}+\frac{\omega_j^2}{\omega^2}+\theta^2\right]^{-1} \tag{3}$$

where $i^2=-1$, θ is the angle between the charged particle velocity and the direction of XTR photon, $\gamma^{-2}=1-\beta^2$, $\beta=v/c$ is the ratio of the particle velocity v and the speed of light c, ω_j and l_j are the plasma frequency and the photon absorption length in the medium, respectively. In the case of a transparent medium, $L_j/l_j\to 0$, the complex formation zone is reduced to the *coherence length* L_j of XTR, which is a real number.

The integration of Eq. (1) in respect to θ^2 can be simplified for the case of regular radiator ($\nu_{1,2}\to\infty$) with media transparent for

E-mail address: Vladimir.Grichine@cern.ch

0168-9002/$ - see front matter © 2012 Elsevier B.V. All rights reserved.
http://dx.doi.org/10.1016/j.nima.2012.09.002

XTR photons, and $n \gg 1$ [11,12]. Then the radiator factor $\langle R^{(n)} \rangle$ reads:

$$\langle R^{(n)} \rangle = 2\sin^2\varphi_1 \frac{\sin^2 n\varphi}{\sin^2\varphi} \overset{n\gg 1}{\to} 2n\sin^2\varphi_1 \sum_k \delta\left(\frac{\varphi}{\pi}-k\right)$$

$$\varphi = \varphi_1+\varphi_2, \quad \varphi_j = \frac{t_j}{4L_j}.$$

The energy spectrum of emitted XTR photons can be expressed as a finite sum:

$$\frac{d\overline{N}_{in}}{\hbar d\omega} = \int_0^{\theta^2_{max}} d\theta^2 \frac{d^2\overline{N}_{in}}{\hbar\, d\omega\, d\theta^2} \simeq \frac{4\alpha n}{\pi\hbar\omega}(C_1+C_2)^2 \cdot \sum_{k=k_{min}}^{k_{max}} \frac{(k-C_{min})}{(k-C_1)^2(k+C_2)^2}\sin^2\left[\frac{\pi t_1}{t_1+t_2}(k+C_2)\right] \quad (4)$$

$$C_{1,2} = \frac{t_{1,2}(\omega_1^2-\omega_2^2)}{4\pi c\omega}$$

$$C_{min} = \frac{1}{4\pi c}\left[\frac{\omega(t_1+t_2)}{\gamma^2}+\frac{t_1\omega_1^2+t_2\omega_2^2}{\omega}\right]$$

where $\hbar$ is Planck's constant. The sum in Eq. (4) is defined by the terms with integer $k \gtrsim k_{min}$ corresponding to the region of $\theta \gtrsim 0$. Therefore k_{min} should be the nearest to C_{min} integer $k_{min} \geq C_{min}$. Each term in the sum of spectrum (4) corresponds to the emitting angle

$$\theta_k^2 = \frac{4\pi c}{\omega(t_1+t_2)}|k-C_{min}|.$$

Then the angle spacing is

$$\Delta\theta^2 = \theta_{k+1}^2-\theta_k^2 = \frac{4\pi c}{\omega(t_1+t_2)}.$$

This value corresponds to the angle bin ($\sqrt{\Delta\theta^2}$) of about 1 mrad for the typical XTR energy of 10 keV generated by charged particle with the Lorentz factor $\sim 10^4$ in the typical radiator with $t_1+t_2 \sim 0.5$ mm. The maximum emitting angle is chosen empirically and corresponds to $k_{max} \sim k_{min}+50$. The sum in Eq. (4) can be used for the simulation of the integral XTR angular distribution at a given XTR energy, since the probability of emitting angle $\theta > \theta_l$, where $l \geq k_{min}$, is proportional to the partial sum (4) starting with l. This algorithm for the preparation of the XTR angular distribution was implemented in the GEANT4 XTR package and available since the GEANT4 9.5 version.

Fig. 1 shows the X-ray transition radiation spectrum measured in the ALICE test-beam environment [13]. The beam consists of electrons with the momentum 2 GeV/c. Since the gap between the XTR radiator (120 polypropylene foils 15 μm thick interspersed with 0.4 mm air gaps) and the detector (MWPC filled with Xe and CO_2 (15%) and pad 0.75×8 cm^2 readout) was about 1.6 m and partly inside a magnetic field (1 T), we simulate also the X-ray synchrotron radiation in the field. In addition, the angular broadening due to the X-ray Rayleigh scattering and the electron beam divergence (few mrad) were taking into account to reproduce the environment of the experimental setup (the solid histogram). Note that the intrinsic transverse resolution, i.e. the ratio of the readout pad thickness to the radiator–detector gap, of this setup was about 5 mrad. The dashed histogram shows the GEANT4 simulation with the simplified XTR angular distribution according to Gaussian sampling with the mean root square angle of $3/\gamma$. The open and solid points are the ALICE experimental data and ALIROOT simulation, respectively [13]. One can see that the advanced algorithm (the solid histogram) for the XTR angular radiation provides better description of the ALICE test-beam experimental data in the range of the distribution tail. For low (<10 keV) XTR energies both GEANT4 simulations underestimate the data and this discrepancy is under investigation.

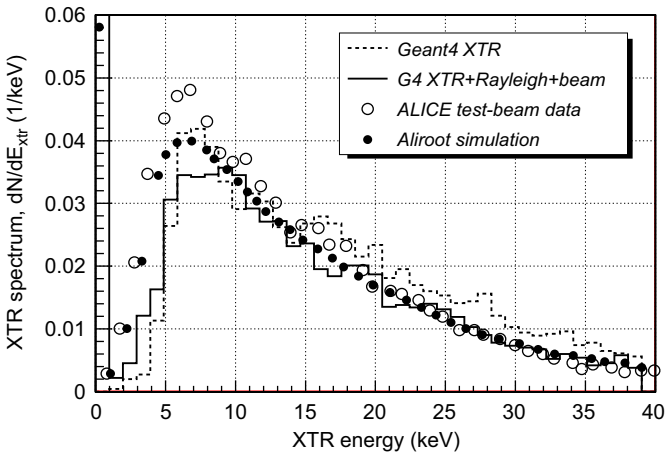

Fig. 1. The X-ray transition radiation spectrum measured in the ALICE test-beam environment. The open and solid points are the ALICE experimental data and ALIROOT simulation, respectively. The solid histogram is the simulation according the XTR angular distribution described here, while the dashed histogram corresponds to the GEANT4 simulation with simplified XTR angular distribution.

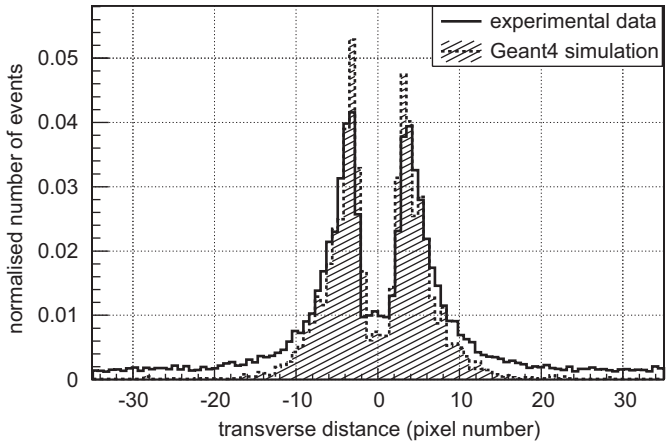

Fig. 2. The transverse distribution of the X-ray transition radiation in the active pixel (20 μm) silicon detector [5]. The histograms [14] show the experimental data (solid curve) and the GEANT4 simulation (dashed curve) according to the algorithm described in this paper.

Fig. 2 shows the transverse distribution of the X-ray transition radiation in the active pixel (20 μm) silicon detector 0.45 mm thick described in detail [5]. The beam consists of electrons with the energy of 5 GeV, the electron multiple scattering in the XTR radiator 15 cm thick was of the order of 0.2 mrad which is comparable with the transverse pixel resolution of ~ 0.3 mrad. The histograms [14] show the experimental data (the solid histogram) and the GEANT4 simulation (the dashed histogram) according to the algorithm described in this paper. The difference between the experiment and the simulation in the tail region is due to the detector noise and the beam background, since the experiment trigger selected few electrons in an event providing flat transverse pedestal.

It should be noted that the XTR theory provides the total XTR energy loss inside XTR radiator or the total flux of the XTR photons after the radiator only. In both cases one cannot reproduce the exact point of the XTR photon origin. In any case the minimal XTR origin point spread along the particle track is about the total coherence length of radiator, L_1+L_2, since this value correspond to the charged particle trajectory part where the XTR photon is created to be a separate particle. It is usually assumed that the longitudinal distribution of the XTR photon origin

position along the particle track is flat. This assumption does not affect practically the XTR energy distribution while the XTR transverse distribution is more sensitive in this sense. One can conclude that, in spite of this theory limitation, the XTR simulation according to the algorithm presented in this paper is in satisfactory agreement with the experimental data, except of the low energy part of Fig. 1 which is under investigation.

Acknowledgment

The author is thankful to S. Furletov for stimulating discussions.

References

[1] B. Dolgoshein, Nuclear Instruments and Methods in Physics Research Section A 326 (1993) 434.
[2] The ATLAS Experiment Technical Design Report, CERN 1998.
[3] The ALICE Transition Radiation Detector Technical Design Report, ALICE TRD 9, CERN/LHCC 2001-021.
[4] M. Bridgida, C. Favuzzi, P. Fusco, et al., Nuclear Instruments and Methods in Physics Research Section A 550 (2005) 157.
[5] J. Furletova, S. Furletov, Nuclear Instruments and Methods in Physics Research Section A 628 (2011) 309.
[6] GEANT4: An Object-Oriented Toolkit for Simulation in HEP, CERN/LHCC 98-44; see also the web site 〈http://geant4.web.cern.ch/geant4/〉.
[7] V.M. Grichine, Physics Letters B 525 (2002) 225.
[8] V.M. Grichine, Nuclear Instruments and Methods in Physics Research Section A 484 (2002) 573.
[9] V.M. Grichine, S.S. Sadilov, Nuclear Instruments and Methods in Physics Research Section A 563 (2004) 299.
[10] J. Apostolakis, S. Giani, V. Grichine, et al., Computer Physics Communications 132 (2000) 241.
[11] G.M. Garibyan, Soviet Physics JETP 32 (1971) 23.
[12] C.W. Fabian, W. Struczinski, Physics Letters B 57 (1975) 483.
[13] R. Bailhache, C. Lippmann, Nuclear Instruments and Methods in Physics Research Section A 563 (2006) 310.
[14] S. Furletov, private communication.